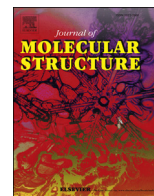




Since January 2020 Elsevier has created a COVID-19 resource centre with free information in English and Mandarin on the novel coronavirus COVID-19. The COVID-19 resource centre is hosted on Elsevier Connect, the company's public news and information website.

Elsevier hereby grants permission to make all its COVID-19-related research that is available on the COVID-19 resource centre - including this research content - immediately available in PubMed Central and other publicly funded repositories, such as the WHO COVID database with rights for unrestricted research re-use and analyses in any form or by any means with acknowledgement of the original source. These permissions are granted for free by Elsevier for as long as the COVID-19 resource centre remains active.



Structural comparison of five new halogenated dihydroquinoline-4(1H)-ones

Wesley F. Vaz ^{a, b, *}, Lidiane J. Michelini ^c, Gerlon A.R. Oliveira ^c, Luciano M. Lião ^c, Caridad N. Perez ^c, Allen G. Oliver ^d, Hamilton B. Napolitano ^{a, e, **}

^a Ciências Exatas e Tecnológicas, Universidade Estadual de Goiás, Anápolis, GO, 75001-970, Brazil

^b Instituto Federal de Educação, Ciência e Tecnologia de Mato Grosso, Lucas do Rio Verde, MT, 78455-000, Brazil

^c Instituto de Química, Universidade Federal de Goiás, Goiânia, GO, 74690-900, Brazil

^d Department of Chemistry and Biochemistry, University of Notre Dame, Notre Dame, IN, 46556, USA

^e Laboratório de Novos Materiais, Centro Universitário de Anápolis, Anápolis, GO, 75083-515, Brazil

ARTICLE INFO

Article history:

Received 3 April 2020

Received in revised form

16 May 2020

Accepted 28 May 2020

Available online 2 June 2020

Keywords:

Dihydroquinoline

Chlorine

Fluorine

Crystal structure

ABSTRACT

Compounds with dihydroquinoline-4(1H)-one nuclei have been reported in the literature for being important in the development of medicines due to their broad spectrum of activities. In this way, the structural knowledge of this class becomes relevant for obtaining new materials with desired biological properties. This study presents the structural elucidation of five halogenated dihydroquinolines, as well as the discussion about the effect on the molecular conformation of the type and position of halogen atom on aromatic rings. Compounds **I** and **IV** differ in halogen substitution on 2-phenyl ring, while compounds **III** and **V** differ in halogen substitution on the benzylidene ring. Moreover, compound **II** has a *para*-substituted 2-phenyl ring in their molecular structure. The crystal packing of all five molecules is mainly ruled by C–H···O and C–H···halogen interactions that form dimers and chains. The shift in position and the kind of the halogen in ring C shows a starring role in the conformation of the studied compounds, and the packaging of these compounds is more susceptible to variations when the halogen position changes.

© 2020 Elsevier B.V. All rights reserved.

1. Introduction

Quinolines are a class of *N*-heterocyclic compounds, also known as benzopyridines, obtained both from natural and synthetic sources. They have attracted great attention in the scientific community being used in several industrial processes, becoming increasingly important in the development of medicines, pesticides and also due to their notable biological activities [1–3]. Among the compounds of this class, we are interested in those with the dihydroquinoline-4(1H)-one moiety; in this way, the recent studies conducted by our research group involve structural elucidation [4–6], anti-cancer properties [7,8] and their potential application as

pesticides [9]. Also, other groups have explored the cytotoxic properties of this class [10–13] and as potential Middle East respiratory syndrome coronavirus (MERS-CoV) inhibitors [14].

The biological activity of a substance is dominated by its properties, which are determined by its chemical structure. Structural elucidation is essential since it allows understanding and proposing explanations for the mechanisms of action at the molecular level, helping to design and develop new materials with desirable biological properties [15,16]. A search in the CSD version 5.41 (November 2019) database showed 132 reported structures with the dihydroquinoline-4(1H)-one nucleus. Furthermore, given the biological potential of these molecules, a need to enlarge elucidated structures of this class will contribute to the applications of dihydroquinoline-4(1H)-ones.

Thus, in this paper, we investigate and report a comprehensive single-crystal analysis of five halogenated dihydroquinoline-4(1H)-ones, namely (*E*)-3-(2-chlorobenzylidene)-2-(2-chlorophenyl)-1-(phenylsulfonyl)-2,3-dihydroquinolin-4(1H)-one (**I**), (*E*)-3-(2-chlorobenzylidene)-2-(4-chlorophenyl)-1-(phenylsulfonyl)-2,3-

* Corresponding author. Ciências Exatas e Tecnológicas, Universidade Estadual de Goiás, Anápolis, GO, 75001-970, Brazil.

** Corresponding author. Ciências Exatas e Tecnológicas, Universidade Estadual de Goiás, Anápolis, GO, 75001-970, Brazil.

E-mail addresses: wesfonseca@gmail.com (W.F. Vaz), hbnapolitano@gmail.com (H.B. Napolitano).

dihydroquinolin-4(1H)-one (**II**), (*E*)-2-(2-bromophenyl)-3-(2-chlorobenzylidene)-1-(phenylsulfonyl)-2,3-dihydroquinolin-4(1H)-one (**III**), (*E*)-2-(2-chlorophenyl)-3-(2-fluorobenzylidene)-1-(phenylsulfonyl)-2,3-dihydroquinolin-4(1H)-one (**IV**) and (*E*)-2-(2-bromophenyl)-3-(2-fluorobenzylidene)-1-(phenylsulfonyl)-2,3-dihydroquinolin-4(1H)-one (**V**). The title compounds were divided into two groups: *chlorinated* and *fluorinated*; and their molecular geometry, intermolecular interactions and crystal packing were all analyzed and discussed in terms of the effect of halogen substitution in their scaffold.

2. Experimental

2.1. Synthesis and crystallization

Compounds **I** to **V** were obtained from sulfonamide chalcones reacted with benzaldehydes in an alkaline reaction environment for 24 h (Scheme 1). The subsequent precipitates were purified by slow recrystallization from dichloromethane and ethanol (4:1), after drying at room temperature.

Nuclear magnetic resonance (NMR) spectra were acquired on a Bruker Avance III 500 spectrometer (Rheinstetten, Germany) operating at 11.75 T with a 5 mm inverse detection three-channel (^1H , ^2H and X-nucleus) BBI probe. The samples (*ca.* 10 mg) were dissolved in 600 μL of deuterated dimethylsulfoxide ($\text{DMSO-}d_6$), containing tetramethylsilane (TMS) as the internal standard. The unambiguous signal assignment was achieved by correlation spectroscopy (COSY), heteronuclear multiple bond correlation (HMBC), heteronuclear single quantum correlation (HSQC), and DEPT-135 experiments, in addition to ^1H and ^{13}C analyses (Table 1).

2.2. Crystallographic characterization

Appropriate single crystals of compounds **I**, **II**, **III**, **IV** and **V** were carefully chosen. They were mounted in a Bruker APEX II CCD diffractometer with graphite-monochromated Mo-K α radiation ($\lambda = 0.71073 \text{ \AA}$), and data were measured at 120 K. Using Olex2 [17], the structure solutions were determined by Direct Methods with SHELXS [18] and refined by full-matrix least-squares on F^2 with SHELXL [19]. All the hydrogen atoms were placed in calculated positions and refined with fixed individual displacement parameters [$U_{\text{iso}}(\text{H}) = 1.2U_{\text{eq}}(\text{C})$ or $1.5U_{\text{eq}}(\text{C})$] according to the riding model (C–H bonds equal 0.93 \AA for aromatic). Ring D in **IIIb** was found to be disordered and modeled over two equal occupancy positions. Lastly, the validation of chemical parameters were made using PARST [20] and PLATON [21]. Data collection and structure refinement details are summarized in Table 2. The structures **I** to **V** were deposited in the Cambridge Crystallographic Data Centre

(CCDC) with the code number 1994320, 1994319, 1994318, 1994317, and 1994316, respectively.

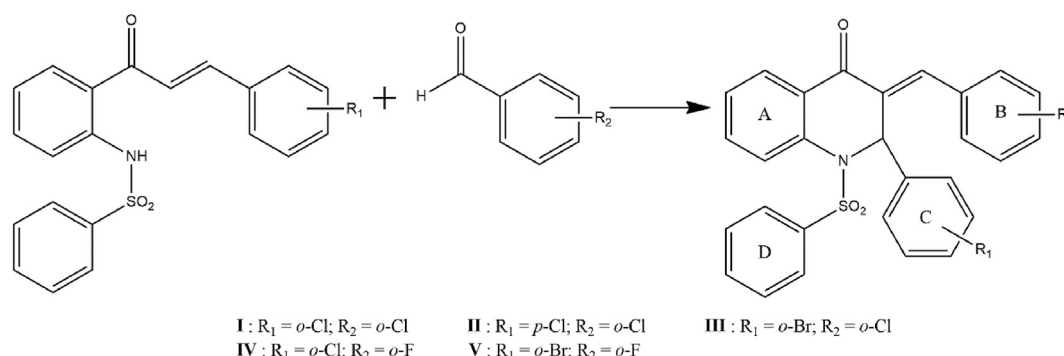
3. Results and discussion

3.1. Spectroscopy characterization

Complete assignment of the signals of ^1H and ^{13}C NMR spectra are presented in Table 1 and the infrared spectra are available in the Support Information. The most deshielded carbon signal, near δ 181 and assigned to carbonyl carbon (C3), was a good starting point to confirm the proposed structure and NMR signal assignments. The strong correlations with C3 in the HMBC experiment ($^3J_{\text{CH}}$) allowed the identification of hydrogens H8, H5, H10 and H1 (Fig. S1). Also, the correlations of these hydrogens with their respective carbons, by HSQC experiment ($^1J_{\text{CH}}$), enabled the assignment of the carbons C10 and C1 (Fig. S2). H10 signal is a broad singlet (Fig. S3) since it presented long-range scalar coupling with the other hydrogens of the benzylidene group. Cross peaks with C1 and H1 in the HMBC spectrum provided information for C22 and C18 assignments (Fig. S1). C9 was identified by its strong correlations with H1, H5, and H7, and weak correlation with H8 (Fig. S1). H16 (and H12 when present) was assigned based on $^3J_{\text{CH}}$ with C10 in HMBC.

The multiplet signal near to δ 7.1 in the ^1H NMR spectrum was assigned to H24/28, since it had an integration of 2 in all the structures and presented $^1J_{\text{CH}}$ and $^3J_{\text{CH}}$ correlations only with the carbons C24/28 and C26, respectively. H25/27 was assigned by a cross peak with H24/28 signal in the COSY experiment (Fig. S4), and their HSQC correlation allowed C25/27 assignment as the carbon signal near to δ 129. H26 and C26 correlation were observed in HSQC and this correlation was supported by correlation with H25/27 in the COSY experiment (Fig. S4). H25/27 shared a strong HMBC cross peak with a carbon signal close to δ 135, assigned as C23. C4 and C23 were differentiated by DEPT-135, in the same way as other quaternary carbons close to tertiary carbons. Thus, all the atoms of the phenyl ring attached to the sulfonamide group were assigned.

The $^3J_{\text{CH}}$ correlations of H10 and H1 were good entry points for the assignments of the rings B and C signals (C11 to C22). In structures **IV** and **V**, the presence of fluorine made the assignments of ring C easier because the neighboring fluorine carbons ($^1J_{\text{CF}} \sim 250 \text{ Hz}$; $^2J_{\text{CF}} \sim 22 \text{ Hz}$; $^3J_{\text{CF}} \sim 9 \text{ Hz}$; $^4J_{\text{CF}} \sim 4 \text{ Hz}$) were observed as doublets, due to coupling between C and F. The hydrogen H16 was assigned by cross peaks observed in HMBC experiment, especially the correlation with C10. The signal for C22 was observed near to δ 123.6 for compounds **III** and **V**, which was markedly shielded when compared to **I** and **IV** (near to δ 143.3). This shielding was due to the attached bromine on the former two compounds and chlorine on the latter two compounds. This kind of strategy allowed a



Scheme 1. Synthesis of compounds **I** to **V**.

Table 1
¹H NMR spectral data assignments for the compounds **I**, **II**, **III**, **IV** and **V** in DMSO-*d*₆.

Compound	I		II		III		IV		V	
	¹ H	¹³ C	¹ H	¹³ C	¹ H	¹³ C	¹ H	¹³ C	¹ H	¹³ C
C1	6.81 (m)	58.4	6.52 (m)	58.9	6.81 (s)	60.6	6.79 (m)	58.6	6.73 (s)	60.7
C2	—	132.1	—	131.3	—	132.3	—	132.1	—	130.0
C3	—	181.2	—	181.1	—	181.2	—	181.2	—	181.1
C4	—	129.3	—	127.4	—	129.6	—	129.3	—	129.2
C5	7.80 (ddd, 7.6; 1.6; 0.5)	127.7	7.80 (ddd, 7.6; 1.6; 0.5)	127.8	7.78 (ddd, 7.6; 1.6; 0.5)	127.6	7.82 (ddd, 7.7; 1.7; 0.4)	127.6	7.80 (dd, 7.6; 1.4)	127.3
C6	7.45 (ddd, 7.6; 7.6; 1.1)	128.5	7.42 (m)	127.8	7.39 (ddd, 7.6; 7.6; 1.1)	128.2	7.46 (m)	128.5	7.45 (ddd, 7.6; 7.6; 1.0)	128.5
C7	7.65 (ddd, 7.6; 7.6; 1.6)	135.3	7.70 (m)	135.4	7.65 (ddd, 7.6; 7.6; 1.6)	135.3	7.65 (m)	135.2	7.65 (m)	135.2
C8	7.41 (m)	128.1	7.65 (m)	127.4	7.37 (ddd, 7.6; 1.1; 0.5)	127.7	7.39 (m)	128.4	7.37 (dd, 8.2; 1.0)	128.6
C9	—	138.1	—	138.1	—	138.1	—	138.1	—	138.0
C10	7.88 (m)	136.2	7.88 (m)	136.1	7.88 (m)	136.2	7.67 (m)	132.4	7.68 (m)	132.4
C11	—	131.1	—	130.8	—	131.2	—	121.0	—	121.0
C12	—	134.5	—	134.9	—	134.5	—	160.7	—	160.5
C13	7.73 (dd, 8.0; 1.2)	130.5	7.72 (dd, 8.0; 1.4)	130.6	7.73 (dd, 8.0; 1.1)	130.5	7.45 (m)	116.5	7.46 (dd, 7.6; 1.1)	116.5
C14	7.54 (m)	132.1	7.56 (ddd, 8.0; 7.70; 1.6)	132.2	7.54 (ddd, 8.0; 7.6; 1.1)	132.1	6.85 (td, 7.7; 1.7)	129.1	6.85 (dd, 7.6; 7.6; 1.5)	129.2
C15	7.35 (m)	127.6	7.40 (m)	127.8	7.44 (ddd, 7.8; 7.6; 1.1)	128.5	7.28 (td, 7.7; 1.2)	125.0	7.28 (ddd, 7.6; 7.6; 1.1)	125.1
C16	6.72 (dd, 7.9; 1.5)	128.9	7.00 (dd, 7.9; 1.6)	128.8	6.72 (dd, 7.8; 1.7)	128.9	7.60 (m)	133.1	7.60 (m)	133.1
C17	—	135.0	—	136.3	—	136.3	—	134.7	—	135.8
C18	6.79 (dd, 7.9; 1.5)	129.8	7.35 (m)	128.9	6.77 (dd, 7.7; 1.5)	130.1	6.76 (dd, 7.7; 1.6)	129.7	6.75 (dd, 7.7; 1.5)	130.1
C19	7.14 (m)	127.5	7.42 (m)	129.5	7.17 (td, 7.7; 1.5)	128.0	7.12 (td, 7.7; 1.4)	127.4	7.15 (td, 7.7; 1.5)	127.9
C20	7.35(m)	130.8	—	133.4	7.25(ddd, 7.9; 7.7; 1.5)	131.0	7.33 (td, 7.7; 1.6)	130.8	7.23 (ddd, 7.9; 7.7; 1.5)	130.9
C21	7.60 (dd, 7.9; 1.2)	131.0	7.42 (m)	129.5	7.77 (dd, 7.9; 1.2)	134.5	7.60 (m)	131.0	7.76 (dd, 7.9; 1.2)	134.6
C22	—	133.3	7.35 (m)	128.9	—	123.6	—	133.4	—	123.7
C23	—	135.6	—	136.0	—	135.4	—	135.6	—	135.5
C24	7.13 (m)	127.4	7.16 (m)	126.6	7.13 (m)	127.6	7.05 (m)	127.7	7.04 (m)	127.5
C25	7.41 (m)	129.2	7.42 (m)	129.3	7.40 (m)	129.1	7.39 (m)	129.0	7.38 (m)	129.0
C26	7.64 (m)	134.0	7.66 (m)	134.1	7.63 (m)	134.0	7.66 (m)	134.1	7.65 (m)	134.1
C27	7.41 (m)	129.2	7.42 (m)	129.3	7.40 (m)	129.1	7.39 (m)	129.0	7.38 (m)	129.0
C28	7.13 (m)	127.4	7.16 (m)	126.6	7.13 (m)	127.6	7.05 (m)	127.7	7.04 (m)	127.5

Table 2
Crystallographic and refinement details for **I**, **II**, **III**, **IV** and **V**.

	I	II	III	IV	V
Chemical formula	C ₂₈ H ₁₉ Cl ₂ NO ₃ S	C ₂₈ H ₁₉ Cl ₂ NO ₃ S	C ₂₈ H ₁₉ BrClNO ₃ S	C ₂₈ H ₁₉ ClFNO ₃ S	C ₂₈ H ₁₉ BrFNO ₃ S
<i>M</i> _r	520.40	520.40	564.86	503.95	548.41
Crystal system, space group	Triclinic, <i>P</i> -1	Monoclinic, <i>P</i> ₂ ₁ / <i>n</i>	Triclinic, <i>P</i> -1	Triclinic, <i>P</i> -1	Monoclinic, <i>P</i> ₂ ₁ / <i>c</i>
Temperature (K)	120	120	120	120	120
<i>a</i> , <i>b</i> , <i>c</i> (Å)	8.0771 (2), 16.4324 (5), 19.2435 (6)	9.8048 (4), 14.2198 (6), 17.2824 (7)	8.0141 (3), 16.6545 (7), 19.3781 (8)	7.9709 (11), 21.980 (3), 24.471 (3)	29.026 (5), 16.304 (3), 15.322 (2)
α , β , γ (°)	109.114 (2), 94.537 (1), 97.435 (1)	90, 95.552 (1), 90	108.605 (1), 95.549 (1), 97.078 (1)	63.784 (2), 81.456 (2), 82.227 (2)	90, 95.775 (3), 90
<i>V</i> (Å ³)	2372.81 (12)	2398.25 (17)	2407.00 (17)	3791.9 (9)	7214 (2)
<i>Z</i>	4	4	4	6	12
μ (mm ⁻¹)	0.39	0.39	1.94	0.27	1.84
Crystal size (mm)	0.17 × 0.17 × 0.09	0.37 × 0.30 × 0.27	0.19 × 0.18 × 0.14	0.19 × 0.14 × 0.08	0.17 × 0.17 × 0.16
<i>T</i> _{min} , <i>T</i> _{max}	0.675, 0.745	0.683, 0.712	0.594, 0.641	0.951, 0.978	0.940, 0.984
No. of measured, independent and observed [<i>I</i> > 2 σ (<i>I</i>)] reflections	35818, 9758, 6875	36054, 5954, 5242	54875, 11976, 9107	68765, 16965, 12459	194960, 18117, 13854
<i>R</i> _{int}	0.045	0.019	0.037	0.046	0.064
(<i>sin</i> θ / λ) _{max} (Å ⁻¹)	0.627	0.668	0.668	0.644	0.670
<i>R</i> [<i>F</i> ² > 2 σ (<i>F</i> ²)], <i>wR</i> (<i>F</i> ²), <i>S</i>	0.038, 0.089, 1.00	0.031, 0.085, 1.04	0.043, 0.101, 1.04	0.040, 0.096, 1.03	0.043, 0.100, 1.04
No. of reflections	9758	5954	11976	16965	18117
No. of parameters	631	316	661	946	946
$\Delta\rho_{max}$, $\Delta\rho_{min}$ (e Å ⁻³)	0.36, -0.42	0.39, -0.38	1.13, -2.61	0.33, -0.36	1.90, -0.84

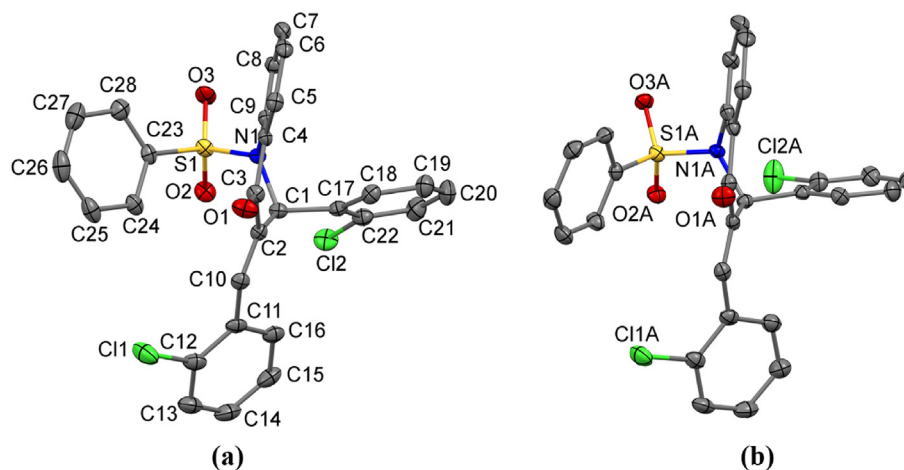


Fig. 1. The two independent molecules of **I** showing the atom-labeling scheme: (a) molecule **Ia**, (b) molecule **Ib**. To clarify, in (b) the labeling scheme shows only non-carbon atoms. The labeling scheme for C atoms in (b) follows the same way as presented in (a). Displacement ellipsoids are drawn at the 50% probability level and H atoms have been omitted.

Table 3
Torsion angles and least-square planes of aromatic rings of **I**, **II**, and **III**.

Molecule	ϕ_1	ϕ_2	ϕ_3	$\angle AB$
Ia	-146.9(3)	145.9(2)	87.46(16)	54.40(7)
Ib	-147.4(2)	168.88(19)	77.35(16)	62.55(7)
II	137.5(2)	167.77(12)	-84.58(13)	60.12(4)
IIIa	-148.9(3)	164.83(2)	-104.43(2)	61.00(9)
IIIb	-147.7(3)	147.28(2)	-87.85(4)	55.62(9)

$$\phi_1 = \text{C2-C10-C11-C12}; \phi_2 = \text{C2-C1-C17-C22}; \phi_3 = \text{N1-S1-C23-C28}.$$

complete assignment of the ^1H and ^{13}C nuclei (see S.I.), and agrees with our previous report [22].

3.2. Crystallographic characterization

3.2.1. Chlorine dihydroquinolinones

Compound **I** belongs to the class of dihydroquinolinones having three substituents groups in its motif. A sulfonylbenzene group attached to N atom; an *ortho*-chlorobenzene attached to C1 atom and a chloro-2-vinylbenzene attached to C2 atom (Scheme 1). Compound **I** crystallizes in the triclinic system ($P\bar{1}$) with two independent molecules in the asymmetric unit (ASU), labeled as **Ia** and **Ib** (Fig. 1). To clarify, in this paper we chose arbitrarily all the molecules within the ASU have *R* configuration about the stereogenic center. To understand the geometrical differences between these molecules their structures have been overlaid using the atoms C1, C3, and C5 as anchor points (Fig. S48). The primary variances noted within these structures are related to the orientations of rings B, C and D with respect to the A ring (defined on Table 3). These variances were measured using the following parameters: the torsion angles: C2-C10-C11-C12 (ϕ_1), C2-C1-C17-C22 (ϕ_2) and N1-S1-C23-C28 (ϕ_3), and the dihedral angle between the planes formed by ring A and ring B ($\angle AB$) (Table 3).

The $\angle AB$ dihedral angle is *ca* 8° larger in **Ib** than in **Ia**, evidencing that the rings in these two molecules have different orientation. This characteristic is also observed in other crystal structures of dihydroquinolinones derivatives [23–25]. Except for compound **II**, these characteristics are the same for all compounds studied here. The orientation of ring B (ϕ_1), could be considered the same in **Ia** and **Ib**, it assumes an *anti-clinal* orientation. Furthermore, the values of ϕ_2 show that ring C assumes an *anti-clinal* and an *anti-periplanar* orientation in **Ia** and **Ib**, respectively, with a difference of 23° . Finally, ϕ_3 shows a *syn-clinal* orientation of ring D

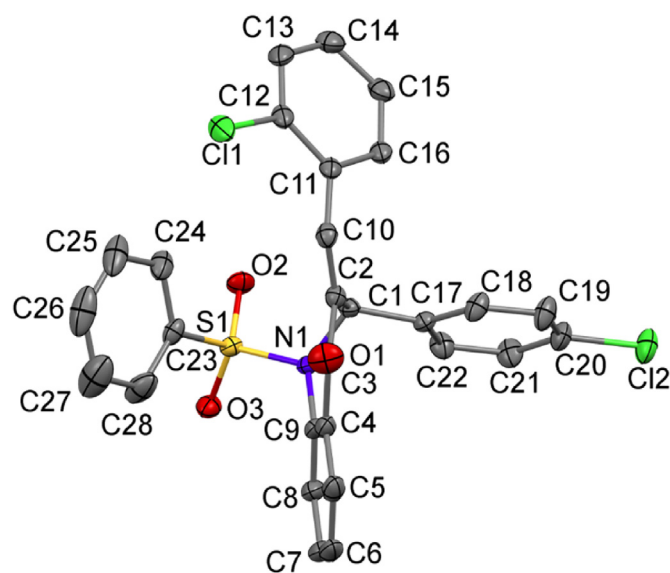


Fig. 2. The molecular structure of **II** showing the atom-labeling scheme. Displacement ellipsoids are drawn at the 50% probability level and H atoms have been omitted.

with a difference of *ca* 10° between the two molecules.

Compound **II**, (Fig. 2), is a positional isomer of **I**, having a chloro-4-vinylbenzene attached to C2 atom (Scheme 1). It is the structure with $\angle AB$ angle smaller than **Ib** and larger than **Ia**. In its molecular structure, unlike **Ia**, ϕ_1 shows that ring B assumes an *anti-clinal* orientation. The change of position of the chlorine atom causes a significant geometric change concerning compounds **I** and **III**. In **II** the rings C and D are oppositely oriented compared with the same rings in the other compounds studied here. The values of ϕ_2 indicate similarity in the molecular set and can be divided into two groups, one containing the molecules **Ib**, **II** and **IIIa** and the other containing the molecules **Ia** and **IIIb**. In compound **II**, ϕ_2 and ϕ_3 assume *anti-periplanar* and a *syn-clinal* orientations, respectively.

Compound **III** differs from **I** only in the presence of the bromo-2-vinylbenzene bonded to the C2 atom (Scheme 1). The two independent molecules in the ASU were labeled as **IIIa** and **IIIb** (Fig. 3). The overlay of these structures indicates a difference of 14° in $\angle AB$ angle for **IIIa** and **IIIb** (Fig. S49). When compounds **I**, **II** and **III** are compared ($\angle AB$ angle), it is possible to distinguish two sets

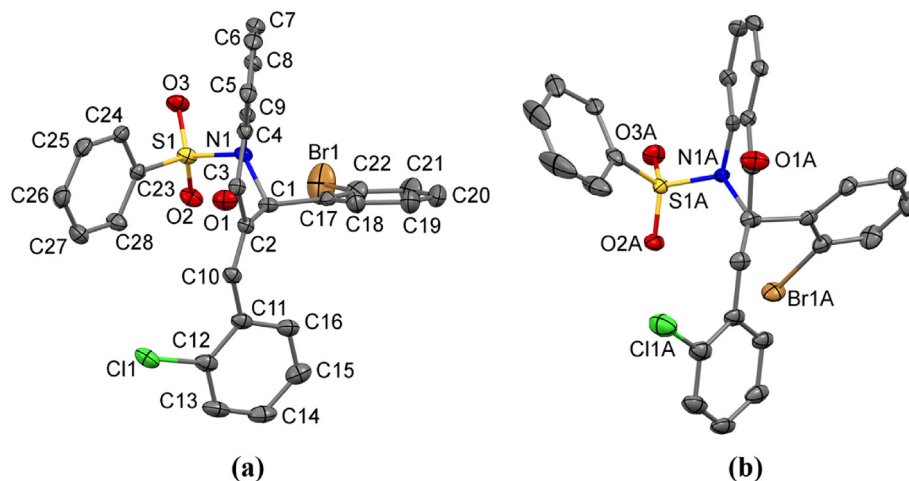


Fig. 3. The two independent molecules of compound **III**, showing the atom-labeling scheme: (a) molecule **IIIa**, (b) molecule **IIIb**. To clarify, in (b) the labeling scheme shows only non-carbon atoms. The labeling scheme for C atoms in (b) follows the same way as presented in (a). Displacement ellipsoids are drawn at the 50% probability level and H atoms have been omitted.

Table 4
Hydrogen-bond geometry (Å, °) of **I**, **II** and **III**.

$D-H\cdots A$	$D-H$	$H\cdots A$	$D\cdots A$	$D-H\cdots A$
I				
C14–H14 \cdots O2A ⁱ	0.95	2.46	3.374 (3)	162
C8A–H8A \cdots O3 ⁱⁱ	0.95	2.36	3.138 (3)	138
C13A–H13A \cdots O2 ⁱ	0.95	2.38	3.326 (3)	175
C27A–H27A \cdots O3A ⁱⁱ	0.95	2.50	3.175 (3)	128
II				
C6–H6 \cdots O2 ⁱⁱⁱ	0.95	2.44	3.3531 (16)	160
III				
C8–H8 \cdots O3A ⁱ	0.95	2.40	3.161 (3)	137
C13–H13 \cdots O2A ^{iv}	0.95	2.31	3.245 (3)	169
C21–H21 \cdots O1A ^v	0.95	2.55	3.458 (4)	159
C25–H25 \cdots O3 ⁱ	0.95	2.50	3.305 (3)	142
C14A–H14A \cdots O2 ^{iv}	0.95	2.46	3.385 (3)	165
C19–H19 \cdots Br1 ⁱⁱⁱ	0.95	2.82	3.626 (3)	143

Symmetry codes: (i) $-x+1, -y+1, -z+1$; (ii) $-x+1, -y, -z+1$; (iii) $x+1, y, z$; (iv) $-x+1, -y+2, -z+1$; (v) $x, y, z+1$.

IIIa molecules. The decreasing of $\angle AB$ angle value regarding chlorine dihydroquinolinones is **Ia**, **IIIb**, **II**, **IIIa**, and **Ib** (Table 3). There is no significant difference between ϕ_1 in the molecules of compounds **I** and **III**, but this torsion in **II** is, *ca* 10° less twisted. The values of ϕ_2 show that ring C assumes an *anti-periplanar* orientation in **IIIa** while in **IIIb** it is *anti-clinal* with a difference of *ca* 17°. ϕ_2 values are similar for **Ib**, **II** and **IIIa** and being *ca* 20° smaller for **Ia** and **IIIb**. The orientation of ring D (ϕ_3) in **IIIa** is *anti-clinal* while in **IIIb** is *syn-clinal* with a difference *ca* 17°.

The crystal structure of these chlorine dihydroquinolinones is stabilized by C–H \cdots O and C–H \cdots halogen hydrogen bonds listed in Table 4. Although these interactions are weak, we are interested in how they affect the packing and if the different substituents on ring C lead to different arrangements. In the molecular packing in the unit cell of compound **I**, two **Ib** molecules are involved in C27A–H27A \cdots O3A interactions leading to the formation of a $R_2^2(12)$ dimer along the *b* axis. Meanwhile, one **Ia** molecule links to

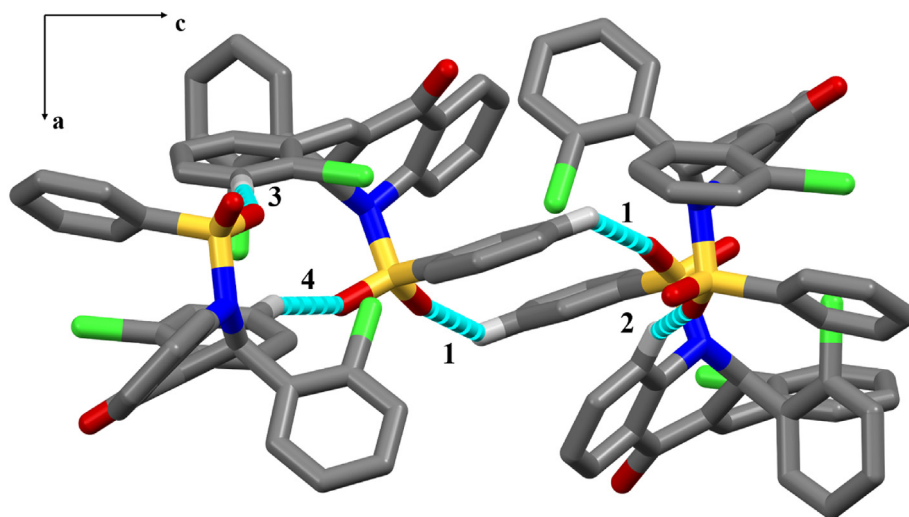


Fig. 4. A partial packing view of **I** showing the dimer formed by C27A–H27A \cdots O3A interaction (1), and the discrete contacts C8A–H8A \cdots O3 (2), C13A–H13A \cdots O2 (3), and C14–H14 \cdots O2A (4). For clarity, H atoms not involved in the motif have been omitted.

with similar values: first with **IIIb** and **Ia**, and second with **Ib**, **II**, and

these dimer, along the *c* axis, through three $D_1^1(2)$ discrete contacts

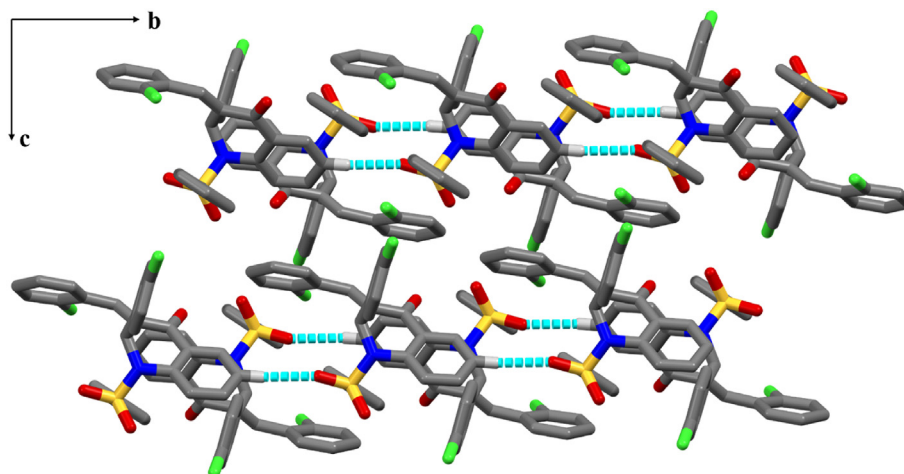


Fig. 5. A partial packing view of **II** showing the chains formed by C6–H6...O2 interaction. For clarity, H atoms not involved in the motif have been omitted.

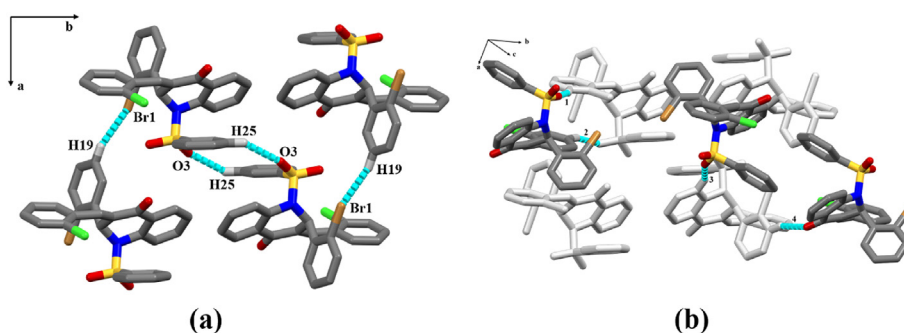


Fig. 6. A partial packing view of **III**, showing the dimer and the chain formed by C25–H25...O3 and C19–H19...Br1 interactions, respectively (a). The discrete contacts C13–H13...O2A (1), C14A–H14A...O2 (2), C8–H8...O3A (3), and C21–H21...O1A (4) join molecules of **IIIa** and **IIIb** in the packing (b); the motif in (a) is presented in (b) in light grey to better visualization. For clarity, H atoms not involved in interactions have been omitted.

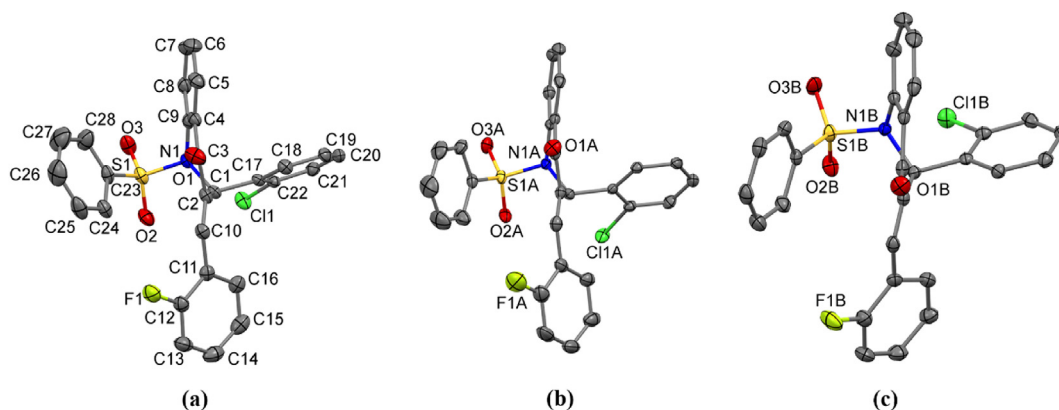


Fig. 7. The three independent molecules of **IV** showing the atom-labeling scheme: (a) molecule **IVa**, (b) molecule **IVb**, and (c) molecule **IVc**. To clarify, in (b) and (c) the labeling scheme shows only non-carbon atoms. The labeling scheme for C atoms in (b) and (c) follow the same way as presented in (a). Displacement ellipsoids are drawn at the 50% probability level and H atoms have been omitted.

[26].: C8A–H8A...O3, C13A–H13A...O2, C14–H14...O2A (Fig. 4).

Because this is a discrete, localized contact, there is no propagation to an extended structure through this contact. The molecular packing of compound **II** is not as varied as that of compound **I**. This arrangement can be described as $C_1^1(8)$ chains that extend along the *a* axis by molecules that are associated through a C6–H6...O2 interaction (Fig. 5). The molecular packing of compound **III** seems

remarkably similar to compound **I**. The differences indicate the carbonyl groups are not related to interactions in the packing of compound **I**. Two molecules of **IIIa** are arranged by C25–H25...O3 interaction as a $R_2^2(12)$ dimer along the *b* axis, and by C19–H19...Br1 interaction as a $C_1^1(6)$ chain along the *a* axis. The molecules of **IIIb** are connected to this arrangement by discrete contacts: C13–H13...O2A, C14–H14A...O2, and C–H8...O3A along

Table 5
Torsion angles and least-square planes of aromatic rings of **IV** and **V**.

Molecule	ϕ_1	ϕ_2	ϕ_3	$\angle AB$
IVa	-141.7(2)	169.45(17)	91.06(19)	58.77
IVb	-153.9(2)	150.24(17)	72.24(16)	49.30
IVc	-150.1(2)	-178.22(16)	75.28(16)	59.71
Va	-157.7(3)	175.3(2)	78.1(2)	44.53
Vb	-144.4(3)	173.7(2)	72.1(2)	62.80
Vc	-149.7(3)	161.1(2)	82.7(2)	52.79

$\phi_1 = C2-C10-C11-C12$; $\phi_2 = C2-C1-C17-C22$; $\phi_3 = N1-S1-C23-C28$.

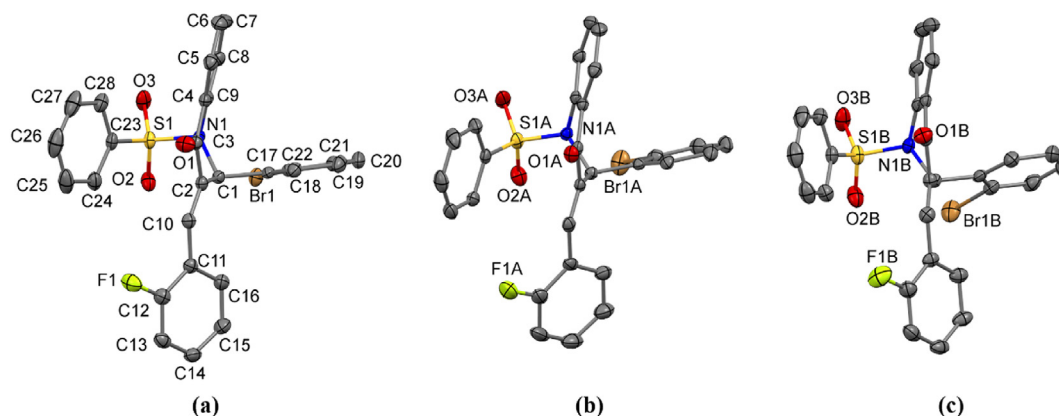


Fig. 8. The three independent molecules of compound **V**, showing the atom-labeling scheme: (a) molecule **Va**, (b) molecule **Vb**, and (c) molecule **Vc**. To clarify, in (b) and (c) the labeling scheme shows only non-carbon atoms. The labeling scheme for C atoms in (b) and (c) follow the same way as presented in (a). Displacement ellipsoids are drawn at the 50% probability level and H atoms have been omitted.

to the *b* axis, while the C21–H21...O1A interaction grows the packing along to the *c* axis. (Fig. 6).

3.2.2. Fluorine dihydroquinolinones

Compound **IV** has an *ortho*-chlorobenzene attached to C1 atom and a fluoro-2-vinylbenzene attached to the C2 atom (Scheme 1). The three independent molecules in ASU were labeled as **IVa**, **IVb** and **IVc** (Fig. 7). As listed in Table 5, these three structures present a variation of 10° in their $\angle AB$ angle being the descending order equal to **IVb**, **IVa**, and **IVc** (Fig. S50). The torsion related to ring B (ϕ_1) is *syn-clinal* oriented for **IVb** and **IVc**, and *anti-clinal* oriented for **IVa**, with a variation of *ca* 12° between them. The values for ϕ_2 show that ring C has more mobility than ring B, with a *ca* 28° of variation in this torsion. The orientation of ring D (ϕ_3) varies *ca* 19°, in **IVa** it is almost perpendicular to SO₂ group while in **IVb** and **IVc** it is almost parallel to O2a and O2b atoms, respectively.

Compound **V** is like compound **IV** but has an *ortho*-bromobenzene attached to C1 atom. The three independent molecules in the ASU were labeled as **Va**, **Vb** and **Vc** (Fig. 8). These molecules present a variation of 18° in their $\angle AB$ angle being the descending order equal to **Va**, **Vc** and **Vb** (Fig. S51). When $\angle AB$ angle values for all fluorine dihydroquinolinones are compared, it is observed a decreasing order **Va**, **IVb**, **Vc**, **IVa**, **IVc**, and **Vb** (Table 5). Just like for chlorine dihydroquinolinones, it is not possible to figure out a clear correlation between the substitution of halogens and the AB ring orientation of these fluorine dihydroquinolinones. The torsion ϕ_1 is *anti-periplanar* oriented in **Va** while in **Vb** and **Vc** it is *anti-clinal*. The values of ϕ_2 show that ring C assumes an *anti-periplanar* orientation in all molecules of compound **V** with a difference of *ca* 14°. The torsion ϕ_3 shows ring D in *syn-clinal* orientation in all molecules of compound **V**, with a change of *ca* 10°. These values, when compared with compound **IV**, shows it having more mobility in the molecule of **IVa**, being *ca* 9° larger than in **Vc**.

The molecular packing in the unit cell of compound **IV** and **V** is stabilized by C–H...O and C–H...halogen hydrogen bonds (Table 6). In compound **IV**, the contacts C5B–H5B...O3B, C18A–H18A...O2A, and C19A–H19A...Cl1A form C₁ⁱ(7) and C₁ⁱ(6) chains along the *a* axis. Molecules of **IVa** are linked through C26B–H26B...O3 and C15–H15...O3A interactions, leading to crystal packing along the *b* axis (Fig. 9a). These motifs (molecules of **IVb** and **IVc**) are attached by the discrete contacts: C14A–H14A...O2B, C14B–H14B...O2A, C27A–H27A...O1, and

Table 6
Hydrogen-bond geometry (Å, °) for compounds **IV** and **V**.

D–H...A	D–H	H...A	D...A	D–H...A
IV				
C5B–H5B...O3B ⁱ	0.95	2.48	3.104 (2)	123
C14A–H14A...O2B ⁱⁱ	0.95	2.47	3.378 (3)	161
C14B–H14B...O2A ⁱⁱⁱ	0.95	2.58	3.518 (3)	168
C15–H15...O3A ^{iv}	0.95	2.57	3.463 (3)	156
C18A–H18A...O2A ^{iv}	0.95	2.57	3.289 (2)	133
C26B–H26B...O3	0.95	2.60	3.326 (2)	134
C27A–H27A...O1 ^v	0.95	2.56	3.238 (2)	129
C19A–H19A...Cl1A ^{iv}	0.95	2.71	3.437 (3)	155
V				
C7A–H7A...O1B	0.95	2.59	3.474 (3)	155
C8A–H8A...F1B	0.95	2.54	3.381 (3)	147
C18A–H18A...O2A ^{vi}	0.95	2.56	3.283 (3)	133
C18–H18...O2 ^{vii}	0.95	2.60	3.256 (2)	131
C26A–H26A...O1B ^{viii}	0.95	2.39	3.335 (3)	171
C14B–H14B...O2	0.95	2.38	3.257 (3)	154
C18B–H18B...O2B ^{ix}	0.95	2.44	3.261 (3)	145
C24A–H24A...O1A ^{viii}	0.95	2.62	3.346 (4)	133
C26–H26...O1 ^x	0.95	2.47	3.256 (4)	140
C27B–H27B...O1A ^{viii}	0.95	2.49	3.357 (3)	152
C27–H27...F1 ^x	0.95	2.52	3.342 (3)	144

Symmetry codes: (i) $x+1, y, z$; (ii) $x+1, y-1, z$; (iii) $x-1, y+1, z$; (iv) $x-1, y, z$; (v) $-x+1, -y+1, -z$; (vi) $x, -y+3/2, +z+1/2$; (vii) $x, -y+3/2, +z-1/2$; (viii) $-x+1, -y+1, -z+2$; (ix) $x, -y+1/2, +z+1/2$; (x) $-x, -y+2, -z+1$.

C14B–H14B...O2A leading the packing to grow along to *c* axis (Fig. 9b).

In the crystal packing of compound **V**, two molecule of **Va** are arranged as dimers through C26–H26...O1, $R_2^2(22)$, and C27–H27...F1, $R_2^2(24)$, interactions. C14B–H14B...O2 interaction attaches those dimers. Along to *a* axis there is a molecular pair formed by the following interactions: C8A–H8A...F1B and C7A–H7A...O1B (Fig. 10). The interaction C18–H18...O2, and

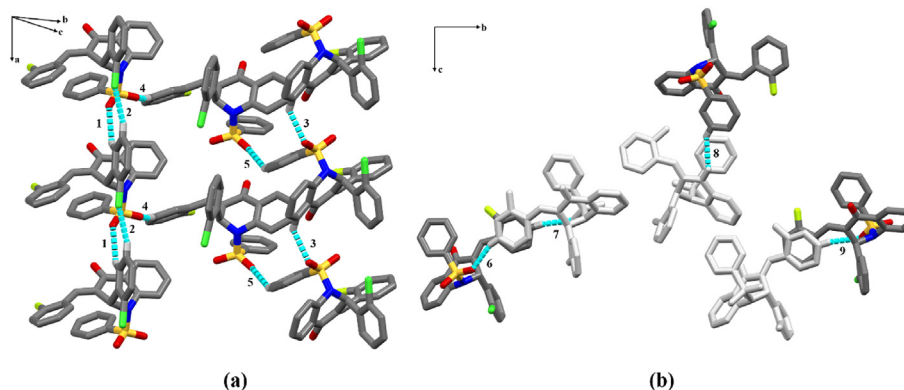


Fig. 9. A partial packing view of **IV** showing (a) the two chains formed by C18A—H18A...O2A (1) and C19A—H19A...C11A (2), and C5—H5B...O3B (3) interactions. In addition, the interactions C15—H15...O3A (4) and C26B—H26B...O3 (5) responsible to connect molecules of **IVa** to the chains. In (b) are shown the discrete contacts C14A—H14A...O2B (6), C14B—H14B...O2A (7), C27A—H27A...O1 (8), C14B—H14B...O2A (9), responsible for grow the packing along the *c* axis. The motif represented in (a), is presented in light grey. For clarity, H atoms not involved in the motif have been omitted.

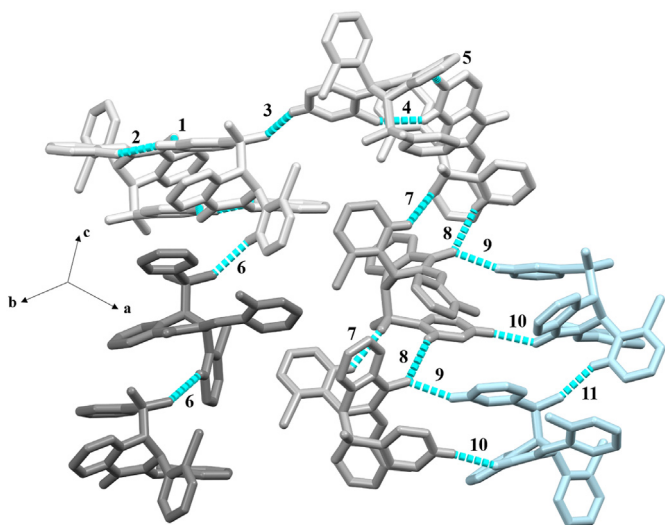


Fig. 10. A partial packing view of **V** showing the dimer and molecular pair in light grey, interactions C26—H26...O1 (1), C27—H27...F1 (2), C14B—H14B...O2 (3), C8A—H8A...F1B (4), nC7A—H7A...O1B (5). The chains formed by C18—H18...O2 (6) (grey); C18A—H18A...O2A (7) and C24A—H24A...O1A (8) (dark grey); and C18B—H18B...O2B (11) (light blue). The interactions C27B—H27B...O1A (9) and C26A—H26A...O1b (10) are discrete and connect two chains. For clarity, H atoms not involved in the motif have been omitted.

C18A—H18A...O2A create two independent $C_1^1(7)$ chains while C24A—H24A...O1A create a $C_1^1(9)$ chain, along to *c* axis. In the same orientation to these chains there is one more $C_1^1(7)$ arrangement formed by C18B—H18B...O2B interaction. This chain connects to others along to *a* axis, via C26A—H26A...O1b and C27B—H27B...O1A interactions (Fig. 10).

4. Final remarks

In this paper we briefly presented a comparison between chlorine and fluorine dihydroquinolinones. Due to the molecular similarities, we discuss the comparison of compounds **I** and **IV**, and compounds **III** and **V**. Concerning **I** and **IV**, the difference is in the halogen at the *ortho* position of ring B, chlorine, and fluorine, respectively. The decreasing order of $\angle AB$ angle is **IVb**, **Ia**, **IVa**, **IVc** and **Ib**. The torsion ϕ_1 in **I** shows a smaller variation when compared to compound **IV**, *ca.* 0.3° and 12°, respectively. Regarding

torsion ϕ_2 , both compounds present similar values (23° for **I** and 19° for **IV**). The torsion angle ϕ_3 in **IV** is larger than **I** (10° and 19°, respectively). Regarding molecular packing, the chlorine compound forms $C_1^1(7)$ and $C_1^1(6)$ chains, while the fluorine compound forms $C_1^1(7)$ chains. All those chains grow along the *a* axis. Finally, discrete contacts join these chains along the *b* and *c* axis.

In contrast, compounds **III** and **V** differ in the halogen in the *ortho* position of ring B, chlorine, and fluorine, respectively. In terms of $\angle AB$ values, the decreasing order is **Va**, **Vc**, **IIIb**, **IIIa**, and **Vb**. The torsion ϕ_1 in **III** is smaller than **V** (1° and 13°, respectively). Regarding the torsion ϕ_2 , both compounds present similar values (17° in **III** and 14° in **V**). Moreover, the torsion ϕ_3 to **III** is larger than **V** (17° and 10°, respectively). These small alterations occur likely due to the change in radius of the halogen atoms. In terms of molecular packing both compounds have $R_2^2(12)$ dimers but in **III** it is related to SO₂ group while in the compound **V** it is related to the carbonyl group. In compound **III** these dimers are arranged along the *c* axis while in compound **V** they are along the *b* axis. Also, the molecular packing in **V** present two $C_1^1(7)$ and one $C_1^1(9)$ chain along the *c* axis. All those observations show that the change in position and kind of halogen atom attached in ring C play a significant role in the conformation of the studied compounds. On the other hand, the packing of these compounds is more susceptible to variations when the substituent position changes.

Declaration of competing interest

The authors declare that they have no known competing financial interests or personal relationships that could have appeared to influence the work reported in this paper.

CRediT authorship contribution statement

Wesley F. Vaz: Conceptualization, Data curation, Formal analysis, Funding acquisition, Investigation, Methodology, Project administration, Supervision, Validation, Visualization, Writing - original draft, Writing - review & editing. **Lidiane J. Micheli:** Data curation, Formal analysis, Investigation, Methodology, Visualization, Writing - original draft, Writing - review & editing. **Gerlon A.R. Oliveira:** Data curation, Formal analysis, Investigation, Methodology, Resources, Validation, Investigation, Writing - original draft, Writing - review & editing. **Luciano M. Lião:** Data curation, Formal analysis, Investigation, Methodology, Resources, Validation, Visualization, Writing - original draft, Writing - review & editing. **Caridad N. Perez:** Data curation, Formal analysis, Investigation,

Methodology, Visualization, Resources, Writing - original draft, Writing - review & editing. **Allen G. Oliver:** Conceptualization, Data curation, Formal analysis, Investigation, Methodology, Resources, Software, Supervision, Validation, Visualization, Writing - original draft, Writing - review & editing. **Hamilton B. Napolitano:** Conceptualization, Data curation, Formal analysis, Funding acquisition, Investigation, Methodology, Project administration, Supervision, Validation, Visualization, Writing - original draft, Writing - review & editing.

Acknowledgements

This study was financed in part by the Coordenação de Aperfeiçoamento de Pessoal de Nível Superior (CAPES, Brazil); Grant ID: 88881.190472/2018-01 - Finance Code 001, Conselho Nacional de Desenvolvimento Científico e Tecnológico and Fundação de Amparo à Pesquisa do Estado de Goiás (FAPEG); Grant ID: 20170267000634.

Appendix A. Supplementary data

Supplementary data to this article can be found online at <https://doi.org/10.1016/j.molstruc.2020.128559>.

References

- [1] S. Jain, V. Chandra, P. Kumar Jain, K. Pathak, D. Pathak, A. Vaidya, Comprehensive review on current developments of quinoline-based anticancer agents, *Arab. J. Chem.* 12 (2019) 4920–4946, <https://doi.org/10.1016/j.arabjc.2016.10.009>.
- [2] A. Felczak, P. Bernat, S. Różalska, K. Lisowska, Quinoline biodegradation by filamentous fungus *Cunninghamella elegans* and adaptive modifications of the fungal membrane composition, *Environ. Sci. Pollut. Res.* 23 (2016) 8872–8880, <https://doi.org/10.1007/s11356-016-6116-4>.
- [3] Y.-M. Zeng, H.-H. Zeng, F.-M. Liu, Synthesis and structure characterization of 1,5-benzothiazepine derivatives bearing quinoline moiety, *J. Heterocycl. Chem.* 53 (2016) 887–893, <https://doi.org/10.1002/jhet.1519>.
- [4] C.A. Moreira, J.M.F. Custódio, W.F. Vaz, G.D.C. D'Oliveira, C. Noda Perez, H.B. Napolitano, A comprehensive study on crystal structure of a novel sulfonamide-dihydroquinolinone through experimental and theoretical approaches, *J. Mol. Model.* 25 (2019) 205, <https://doi.org/10.1007/s00894-019-4091-7>.
- [5] L.J. Michelini, W.F. Vaz, G.D.C. D'Oliveira, C.N. Pérez, H.B. Napolitano, Analysis of two novel 1–4 quinolinone structures with bromine and nitrobenzyl ligands, *J. Mol. Model.* 25 (2019) 55, <https://doi.org/10.1007/s00894-019-3937-3>.
- [6] L. Michelini, W. Vaz, L. Naves, C. Pérez, H. Napolitano, Synthesis, characterization and conformational analysis of two novel 4(1H)-Quinolinones, *J. Braz. Chem. Soc.* 31 (2020) 66–78, <https://doi.org/10.21577/0103-5053.20190124>.
- [7] G.D.C. d'Oliveira, J.M.F. Custódio, A.F. Moura, H.B. Napolitano, C.N. Pérez, M.O. Moraes, L. Próka, P. Perjési, Different reactivity to glutathione but similar tumor cell toxicity of chalcones and their quinolinone analogues, *Med. Chem. Res.* 28 (2019) 1448–1460, <https://doi.org/10.1007/s00044-019-02384-8>.
- [8] W.F. Vaz, J.M.F. Custódio, G.D.C. D'Oliveira, B.J. Neves, P.S.C. Junior, J.T.M. Filho, C.H. Andrade, C.N. Perez, E.P. Silveira-Lacerda, H.B. Napolitano, Dihydroquinoline derivative as a potential anticancer agent: synthesis, crystal structure, and molecular modeling studies, *Mol. Divers.* (2020), <https://doi.org/10.1007/s11030-019-10024-x>.
- [9] W.F. Vaz, G.D.C. D'Oliveira, C.N. Perez, B.J. Neves, H.B. Napolitano, Machine learning prediction of the potential pesticide applicability of three dihydroquinoline derivatives: syntheses, crystal structures and physical properties, *J. Mol. Struct.* 1206 (2020) 127732, <https://doi.org/10.1016/j.molstruc.2020.127732>.
- [10] J. Jean, D.S. Farrell, A.M. Farrelly, S. Toomey, J.W. Barlow, Design, synthesis and evaluation of novel 2,2-dimethyl-2,3-dihydroquinolin-4(1H)-one based chalcones as cytotoxic agents, *Heliyon* 4 (2018), e00767, <https://doi.org/10.1016/j.heliyon.2018.e00767>.
- [11] A. Pejović, J. Drabowicz, M. Cieslak, J. Kazmierczak-Baranska, K. Królewska-Golińska, Synthesis, characterization and anticancer activity of novel ferrocene containing quinolinones: 1-Allyl-2-ferrocenyl-2,3-dihydroquinolin-4(1H)-ones and 1-allyl-2-ferrocenylquinolin-4(1H)-ones, *J. Organomet. Chem.* 873 (2018) 78–85, <https://doi.org/10.1016/j.jorgchem.2018.08.004>.
- [12] J. Koszok, T. Bartosik, J. Wojciechowski, W.M. Wolf, A. Janecka, J. Drogosz, A. Dlugosz, U. Krajewska, M. Mirowski, T. Janecki, Synthesis of 3-Methylidene-1-tosyl-2,3-dihydroquinolin-4(1H)-ones as potent cytotoxic agents, *Chem. Biodivers.* 15 (2018), e1800242, <https://doi.org/10.1002/cbdv.201800242>.
- [13] L. Politanskaya, T. Rybalova, O. Zakharova, G. Nevinsky, E. Tret'yakov, p-Toluenesulfonic acid mediated one-pot cascade synthesis and cytotoxicity evaluation of polyfluorinated 2-aryl-2,3-dihydroquinolin-4-ones and their derivatives, *J. Fluor. Chem.* 211 (2018) 129–140, <https://doi.org/10.1016/j.jfluchem.2018.04.005>.
- [14] J.H. Yoon, J.Y. Lee, J. Lee, Y.S. Shin, S. Jeon, D.E. Kim, J.S. Min, J.H. Song, S. Kim, S. Kwon, Y. Jin, M.S. Jang, H.R. Kim, C.M. Park, Synthesis and biological evaluation of 3-acyl-2-phenylamino-1,4-dihydroquinolin-4(1H)-one derivatives as potential MERS-CoV inhibitors, *Bioorg. Med. Chem. Lett.* 29 (2019) 126727, <https://doi.org/10.1016/j.bmcl.2019.126727>.
- [15] R. Todeschini, V. Consonni, P. Gramatica, *Chemometrics in QSAR*, in: S. Brown, R. Tauler, R. Walczak (Eds.), *Compr. Chemom.* 4, Elsevier, Oxford, 2009, pp. 129–172.
- [16] J.P. a Martins, M.M.C. Ferreira, Qsar modeling: a new open source computational package to generate and validate qsar models, *Quim. Nova* 36 (2013), <https://doi.org/10.1590/S0100-40422013000400013>, 554–U250.
- [17] O.V. Dolomanov, L.J. Bourhis, R.J. Gildea, J.A.K. Howard, H. Puschmann, OLEX2: a complete structure solution, refinement and analysis program, *J. Appl. Crystallogr.* 42 (2009) 339–341, <https://doi.org/10.1107/S0021889808042726>.
- [18] G.M. Sheldrick, A short history of SHELX, *Acta Crystallogr. Sect. A Found. Crystallogr.* 64 (2008) 112–122, <https://doi.org/10.1107/S0108767307043930>.
- [19] G.M. Sheldrick, Crystal structure refinement with SHELXL, *Acta Crystallogr. C* 71 (2015) 3–8, <https://doi.org/10.1107/S2053229614024218>.
- [20] M. Nardelli, Parst 95 – an update to PARST : a system of Fortran routines for calculating molecular structure parameters from the results of crystal structure analyses, *J. Appl. Crystallogr.* 28 (1995), <https://doi.org/10.1107/S0021889895007138>, 659–659.
- [21] A.L. Spek, Single-crystal structure validation with the program PLATON, *J. Appl. Crystallogr.* 36 (2003) 7–13, <https://doi.org/10.1107/S0021889802022112>.
- [22] G. d'Oliveira, A. Moura, M. de Moraes, C. Perez, L. Lião, Synthesis, characterization and evaluation of in vitro antitumor activities of novel chalcone-quinolinone hybrid compounds, *J. Braz. Chem. Soc.* 29 (2018) 2308–2325, <https://doi.org/10.21577/0103-5053.20180108>.
- [23] J.H. Kim, H.W. Ryu, J.H. Shim, K.H. Park, S.G. Withers, Development of new and selective trypanosoma cruzi trans-sialidase inhibitors from sulfonamide chalcones and their derivatives, *Chembiochem* 10 (2009) 2475–2479, <https://doi.org/10.1002/cbic.200900108>.
- [24] H. Ma, X. Zhou, D. Wei, J. Cao, C. Shi, Y. Fan, G. Huang, KHCO 3 - and DBU-promoted cascade reaction to synthesize 3-Benzyl-2-phenylquinolin-4(1H)-ones, *Chem. Asian J.* 11 (2016) 2829–2833, <https://doi.org/10.1002/asia.201600901>.
- [25] M.R.C. de Castro, R.F. Naves, A. Bernardes, C.C. da Silva, C.N. Perez, A.F. Moura, M.O. de Moraes, F.T. Martins, Tandem chalcone-sulfonamide hybridization, cyclization and further Claisen–Schmidt condensation: tuning molecular diversity through reaction time and order and catalyst, *Arab. J. Chem.* 13 (2020) 1345–1354, <https://doi.org/10.1016/j.arabjc.2017.11.005>.
- [26] J. Grell, J. Bernstein, G. Tinhofer, Graph-set analysis of hydrogen-bond patterns: some mathematical concepts, *Acta Crystallogr. Sect. B Struct. Sci.* 55 (1999) 1030–1043, <https://doi.org/10.1107/S0108768199007120>.